



www.sciencemag.org/cgi/content/full/science.1232253/DC1

Supplementary Materials for

Phosphorylation of Dishevelled by Protein Kinase RIPK4 Regulates Wnt Signaling

XiaoDong Huang, James C. McGann, Bob Y. Liu, Rami N. Hannoush, Jennie R. Lill, Victoria Pham, Kim Newton, Michael Kakunda, Jinfeng Liu, Christine Yu, Sarah G. Hymowitz, Jo-Anne Hongo, Anthony Wynshaw-Boris, Paul Polakis, Richard M. Harland, Vishva M. Dixit*

*To whom correspondence should be addressed. E-mail: dixit@gene.com

Published 31 January 2013 on *Science* Express
DOI: 10.1126/science.1232253

This PDF file includes

Materials and Methods
Figs. S1 to S12
Table S1
Full References

Materials and Methods

Plasmids, antibodies, recombinant proteins, and reagents

RIPK4-Myc cDNA was synthesized (Blue Heron) and cloned into pEF2 (Invitrogen). DVL2-FLAG-Myc, DVL2-GFP, RIPK4-GFP plasmids were from Origene. Mutants were generated with a QuickChange Site-Directed Mutagenesis kit (Stratagene). Antibodies recognized RIPK4 (Novus clone 2G3), actin, PKC- β , DVL2, DVL3, phospho-LRP6-Ser1490, LRP6, β -catenin, GSK3- β , or AXIN1 (Cell Signaling Technology), GSK3 (Millipore), HA or FLAG (Sigma), Myc (US Biologicals), DVL1 or DVL2 (Santa Cruz Biotech), PKC- δ (BD Biosciences), and DVL2 phospho-Ser298 or DVL2 phospho-Ser480 (ProSci, Epitomics, Genentech). Other reagents were Wnt3a (Genentech and R & D systems), anti-FLAG and anti-HA beads (Sigma), and calf intestinal alkaline phosphatase (New England Biolabs).

Cell culture and transfection

MEFs, HeLa, 786-O, Hs578T, 293T, and 293 cells transfected stably with a TOPbrite firefly luciferase Wnt reporter and pRL-SV40 Renilla luciferase (Promega) were cultured in DMEM media with 10% fetal bovine serum (FBS; Sigma). PA-1 cells were cultured in 50:50 high-glucose DMEM and Ham's F12 with 10% FBS. COV434 and A2780 cells were cultured in RPMI-1640 with 10% FBS. Plasmids were transfected with Fugene 6 (Roche) or Lipofectamine 2000 (Invitrogen). siRNAs (Dharmacon or Ambion) listed in Supplemental Table 1 were transfected using Lipofectamine RNAiMax (Invitrogen).

Xenopus

Xenopus laevis eggs were fertilized *in vitro* for animal caps or whole mount *in situ* hybridization (14). α Gal, *Xwnt8*, and *Ripk4* RNAs for embryo injection were transcribed *in vitro* with the mMessage Kit (Ambion) and SP6 polymerase. *X. laevis Ripk4* clone BC043634 was from Open Biosystems. Morpholinos for *Ripk4* (GeneTools LLC) were *Ripk4*-MO1: 5' GGA CGC GCC CTC CTT ATC CAC CAT A (injected at 30ng/blastomere), and *Ripk4*-MO2: 5' TAA TGT CAC CGC CGC GCC CCC GAG T (injected at 60ng/blastomere). Antisense digoxigenin-labeled *Engrailed2* and *Chordin* probes were synthesized *in vitro*. RT-PCR primers were *Xnr3*: 5'GTT TAT CTC CCC ACT GAT GGC GAT G, 5'GCT TTG GAC GGT ATC AGA TTC CTG; *Epidermal Keratin*: 5'CAC CAG AAC ACA GAG TAC, 5'CAA CCT TCC CAT CAA CCA; *Xbra*: 5'GGA TCG TTA TCA CCT CTG, 5'GTG TAG TCT GTA GCA GCA; and *Ornithine Decarboxylase (ODC)*: 5'GGG CTG GAT CGT ATC GTA GA, 5'TGC CAG TGT GGT CTT GAC AT.

Western blotting and immunoprecipitations

Cytosolic β -Catenin was determined after depleting cadherin-associated β -catenin with ConA-Sepharose (GE Healthcare). To detect phosphorylated DVL2, cells were lysed in NP40 buffer (1% NP-40, 120 mM NaCl, 50 mM Tris-HCl pH 7.4, 1 mM EDTA pH 7.4) containing 6 M urea, plus protease and phosphatase inhibitors. Whole cell lysates were immunoprecipitated with DVL2 antibody (Cell Signaling Technology) overnight and then anti-rabbit IgG beads (Ebioscience) for 2 h. The beads were washed extensively with high salt buffer (20 mM HEPES pH 7.9, 1.5 mM MgCl₂, 420 mM NaCl, 0.2 mM EDTA, 25% glycerol) and then low salt buffer (20 mM Tris pH 7.4, 300 mM NaCl, 0.2 mM EDTA, 20% glycerol, 0.1% NP40). Eluted

DVL2 protein was probed with phospho-specific DVL2 antibodies and HRP-conjugated anti-rabbit trueblot antibody (eBiosciences).

Recombinant RIPK4 kinase domain

Human RIPK4 residues 2-300 (wild-type or mutant K51R) were cloned into a modified pAcGP67 baculovirus transfer vector (BD Pharmingen) containing an N-terminal His6 tag followed by a Tobacco Etch Virus (TEV) protease site and a C-terminal FLAG tag. Both constructs contained a fortuitous mutation (G²⁶⁸R) that did not affect kinase activity. RIPK4 protein expressed in Sf9 cells was purified at 4°C. Cells from a 5 L culture were re-suspended in lysis buffer (50mM Tris-HCl pH 8.0, 0.3M NaCl, 0.5mM TCEP, 5% glycerol, 50mM NaF, 5mM imidazole, plus Roche complete protease inhibitors cocktail EDTA-free), microfluidized, and centrifuged. Soluble RIPK4 was affinity purified with Ni-NTA Superflow resin (Qiagen). The column was washed in buffer A (25mM Tris-HCl pH 8, 1M NaCl, 5% glycerol, 0.5mM TCEP, 20mM imidazole) and eluted with buffer A containing 250mM imidazole. The His6 tag was removed by overnight dialysis with TEV protease in buffer B (20mM Tris-HCl pH 8.0, 0.2 M NaCl, 0.5 mM TCEP, 5% glycerol). Uncleaved material was removed by passage over a Ni-NTA Superflow column. The cleaved material was further purified using size exclusion chromatography with an S-75 column (GE Healthcare) in buffer C (20mM Tris-HCl pH 8.0, 150mM NaCl, 0.5mM TCEP, 5% glycerol).

***In vitro* kinase assays**

DVL2-PDZ-FLAG (DVL2 residues 267-353, either wild-type or mutant S298A) and DVL2-DEP-FLAG (DVL2 residues 436-505, either wild-type or mutant S480A) were expressed using high-yield wheat germ extract (Promega) and then immunoprecipitated with anti-FLAG M2

beads overnight. The washed beads were used for *in vitro* kinase assays. Briefly, beads were mixed with 0.1 µg of RIPK4 kinase domain (wild-type or mutant K51R), 40 µM ATP (Promega), and 30 µCi γ -³²P-ATP (Perkin Elmer) in kinase buffer (Cell Signaling Technology). Reactions were performed at room temperature for 1 h.

TaqMan, RNA sequencing and Microarray analyses

RNA was extracted with a Qiagen RNeasy kit. TaqMan primers and probes were from Applied Biosystems, and reactions were performed in an ABI 7500 Real Time PCR System with Sequence Detection Software v1.4 (Applied Biosystems). *GAPDH* mRNA levels were used for sample normalization.

Transcriptome sequencing (RNA-seq) of PA-1 cells transfected with empty vector, RIPK1, RIPK2, RIPK3, or RIPK4 was performed on the Illumina Genome Analyzer IIX Platform using a standard paired-end protocol. On average, 20–30 million 75 base pair (bp) reads were obtained per sample. The RNA-seq reads were first aligned to ribosomal RNA sequences to remove potential ribosomal reads. The remaining reads were aligned to the human reference genome (NCBI Build 37) using GSNAP (15), allowing a maximum of 5 mismatches per 75 bp sequencing end. Gene expression levels were quantified by tallying the number of reads mapped to the exons of each RefSeq gene, and adjusting for library size using DEseq (16). For clustering and correlation analysis, variance-stabilized expression values were derived using DEseq, and genes with substantial changes in the treatment groups compared with the vector group (at least two-fold difference and more than 20 reads mapped to the gene in at least one sample) were selected. Hierarchical clustering was performed using euclidean distance as the

distance measure and complete linkage as the agglomeration method. Pair-wise Pearson's correlation coefficients were calculated between samples.

RIPK4 mRNA expression in Fig. 4A was extracted from the Gene Logic (Gaithersburg, MD) expression database of Affymetric Human Genome U133 Plus 2.0 data, representing 319 colorectal samples (211 normals and 108 tumors), 205 ovarian samples (122 normals and 83 normals), and 61 skin samples (51 normals and 10 tumors). Expression summary values for all probesets were calculated using the RMA algorithm as implemented in the affy package from Bioconductor. Student's t-tests were performed to assess the statistical significance of the differences between groups.

Quantitative analysis of DVL2 phosphorylation sites by RIPK4

A SILAC experiment was performed as described (17). Briefly, 293T cells were cultured in DMEM SILAC media (Thermo) supplemented with 10% dialyzed FBS (Invitrogen), plus 50 µg/mL lysine +8, 40 µg/mL arginine +10 (Sigma) (heavy media), or regular 50 µg/mL lysine, 40 µg/mL arginine (Sigma) (light media) for more than 10 days. Labeling efficiency was verified by mass spectrometry. 500 µg of DVL2-FLAG-Myc was transfected into 2×10^8 293T cells, along with 500 µg of RIPK4-FLAG (heavy media), or 500 µg of RIP4-K51R-FLAG (light media) for 48 h. Cells were lysed in NP40 buffer. Equal amounts of the two lysates were mixed and immunoprecipitated with anti-FLAG beads. Samples from the immunoprecipitation were digested with trypsin at 37°C overnight and phosphopeptides enriched using TiO₂. The resulting phosphopeptide mixture was injected onto a 0.1 × 100 mm column packed with 1.7 µm BEH-130 C18 using a NanoAcquity UPLC (Waters) and introduced to a LTQ-Orbitrap mass

spectrometer (ThermoFisher Scientific) through an ADVANCE electrospray ionization source. Peptides were analyzed in data dependent top8 mode, with a full MS scan collected in the FTMS at 60,000 resolution and MS/MS collected in the ion trap on the top 8 most abundant species.

Generation of DVL2-expressing MEFs

DVL2-FLAG (wild-type and mutants) was cloned into pLenti6.3/V5-TOPO (Invitrogen). 5 µg of expression plasmid was mixed with Δ8.9 and VSVG at a molar ratio of 1:2.3:0.2, and transfected into HEK293T cells for 48 h. Filtered virus particles were used to infect *Dvl1*^{-/-} *Dvl2*^{-/-} *Dvl3*^{+/+} MEFs. The cells were then infected with lentiviral particles expressing *Dvl3* shRNA (Open Biosystems). The resulting cells were maintained in DMEM media containing 10% FBS, 2 µg/mL puromycin, and 10 µg/mL blasticidin.

Immunofluorescence microscopy

HeLa cells were transfected with DVL2-FLAG and RIPK4-GFP for 24-36 h. The cells were washed with PBS, fixed in 4% paraformaldehyde at room temperature for 25 min, washed again with PBS, and permeabilized with 0.3% Triton X-100 for 10 min. After blocking in 10% horse serum for 30 min, cells were stained with anti-FLAG antibody in 10% normal horse serum / 0.3% Triton X-100 for 1 h. Bound antibody was revealed with Alexa568-conjugated anti-mouse antibody for 45 min. Cover slips were washed with PBS and mounted on microscope slides. Images were acquired on a Zeiss AxioImager.Z1 microscope (Intelligent Imaging Innovations) equipped with a CoolSnapHQ-cooled CCD camera (Roper Scientific) and a 63× PlanApochromat, NA 1.4 objective. Between 10-16 z sections at 0.3 µm intervals were acquired. Images were processed with Slidebook 4.2 software (Intelligent Imaging Innovation). Contrasts were adjusted identically for each series of panels.

Xenografts

NTERA-2 and HCT116 cells were cultured in McCoy's medium with 15% FBS. Cells were incubated with *RIPK4* shRNA-expressing lentiviral particles (Sigma) at a multiplicity of infection (MOI) of 2-3. Infected cells were cultured in 1 µg/mL puromycin the next day. Resistant cells were trypsinized, washed, resuspended in HBSS:matrigel (1:1), and injected subcutaneously into the left flank of nude mice (~ 0.5 million cells per mouse). Tumor volumes were measured weekly.

Supplementary Figure 1. Expression of RIPK4 in 293T cells upregulates Wnt target genes.

RIPK4 overexpression in 293T cells increases *CCND1*, *LEF1*, *JUN*, *MYC*, and *TCF7* mRNA expression in 293T cells. RNA was extracted at 48 h after transfection for PathwayFinder PCR array analysis.

Supplementary Figure 2. Expression of RIPK4 in PA-1 cells upregulates Wnt target genes.

Graphs show relative expression of four representative Wnt target genes in PA-1 cells transfected with empty vector, RIPK1, RIPK2, RIPK3, or RIPK4 for 48 h. Relative mRNA levels were determined by RNA sequencing.

Supplementary Figure 3. RIPK4 requires a functional kinase domain to activate the Wnt pathway.

A. Expression of a TOPbrite luciferase reporter in 293 cells transfected with empty vector, wild-type RIPK4, or K51R mutant RIPK4 for 48 h. Error bars represent the s.e.m. of triplicate measurements. Results are representative of 3 independent experiments.

B. Western blots show wild-type but not catalytically inactive RIPK4 increases cytosolic β -catenin in 293T cells.

Supplementary Figure 4. Wnt pathway activation by RIPK4 occurs independently of PKC.

A. Endogenous PKC- β and PKC- δ co-immunoprecipitated with RIPK4-FLAG or RIPK4 K52R-FLAG transfected into 293T cells. Non-specific bands (*).

B. Western blots show 293T cells depleted of PKC isoforms accumulate cytosolic β -catenin when they overexpress RIPK4. Cells were transfected with control (Ctrl) or PKC siRNAs and RIPK4-Myc for 48 h.

Supplementary Figure 5. Depletion of RIPK4 compromises Wnt signaling in 293T cells.

A. Western blots show RIPK4 depletion from 293T cells decreases Wnt3a-induced accumulation of cytosolic β -catenin. Cells were infected with lentivirus expressing a RIPK4 or control (Ctrl) shRNA, and then transfected with *RIPK4* or control siRNAs, respectively, prior to treatment with 150 ng/ml Wnt3a. Numbers indicate the relative intensity of the β -catenin bands as determined by densitometry.

B. Expression of a TOPBrite luciferase reporter in 293T cells treated with Wnt3a for 3 h is decreased by RIPK4 depletion. Error bars represent the s.e.m of triplicate measurements.

C-D. Expression of Wnt target genes *AXIN2* and *APCDD1* in 293T cells treated with Wnt3a for 10 h is decreased by RIPK4 depletion. Error bars represent the s.e.m of 3 independent experiments.

P-values in B-D were determined by student t-test.

Supplementary Figure 6. Depletion of RIPK4 from 786-O, Hs.578T, and Panc-1 cells has no effect on Wnt3a-induced accumulation of cytosolic β -catenin.

Western blots show that accumulation of cytosolic β -catenin in response to treatment with Wnt3a is not impaired in all cell lines depleted of RIPK4. Ctrl, control.

Supplementary Figure 7. Modulation of Wnt signaling in *Xenopus* embryos by *Ripk4*.

RT-PCR analysis of *Xwnt8*-induced expression of *Xnr3* in *Xenopus* animal cap cells injected with *Ripk4* morpholinos distinct from those used in Fig. 2C. RNA was prepared from whole embryos (stage 10.5) or animal caps after blastomeres were injected at the two-cell stage. Whole embryo RNA amplified without reverse transcriptase (RT) served as a negative control. RT-PCR of *epidermal keratin* and *ornithine decarboxylase (ODC)* confirmed RNA integrity.

Supplementary Figure 8. DVLs and LRP6 are required for RIPK4 overexpression to cause the accumulation of cytosolic β -catenin.

A. Western blots show depletion of DVL1-3 or LRP6 from 293T prevents the accumulation of cytosolic β -catenin caused by transfection of RIPK4-Myc.

B. Expression of a TOPbrite luciferase reporter in 293 cells depleted of the Wnt pathway components indicated and transfected with RIPK4 for 48 h. Error bars represent the s.e.m. of triplicate measurements. Results are representative of 3 independent experiments.

C. Co-immunoprecipitation of RIPK4-Myc and DVL2-FLAG expressed with rabbit reticulocyte and wheat germ *in vitro* translation systems, respectively.

Supplementary Figure 9. Phosphorylation of DVL2 Ser298 and Ser480 by RIPK4.

A. DVL2-FLAG phosphopeptides enriched in 293T cells expressing RIPK4-FLAG. Cells were transfected with DVL2-FLAG and RIPK4-FLAG (wild-type or mutant K51R) for 48 h. Cells expressing wild-type RIPK4 were cultured in $^{13}\text{C}_6$ -lysine, $^{15}\text{N}_2$ -arginine “heavy” medium, whereas cells expressing RIPK4 K51R were cultured in standard “light” medium. Pooled lysates were immunoprecipitated with anti-FLAG beads and analyzed by mass spectrometry.

B. DVL proteins from different species show conservation of Ser298 and Ser480 in human DVL2.

C. Western blots show the specificity of the anti-phospho-Ser298 DVL2 and anti-phospho-Ser480 DVL2 antibodies. 293T cells transfected were transfected with the construct indicated for 48 h. Non-specific bands (*).

D. Western blots show overexpression of RIPK4-Myc in 293T cells increases phosphorylation of DVL2-FLAG Ser298 and Ser480. Where indicated, whole cell lysates were treated with calf intestinal alkaline phosphatase (CIP).

E. Immunoprecipitation and western blotting of DVL2 in 293T cells stably expressing control (Ctrl) or *RIPK4* shRNAs and treated with 200 ng/mL Wnt3a. Non-specific bands (*).

F. Cytosolic β -catenin abundance in *Dvl*-null MEFs reconstituted with empty vector or DVL2 (wild-type or mutant S298A S480A) and treated with Wnt3a.

Supplementary Figure 10. RIPK4 expression redistributes DVL2 into puncta in HeLa cells.

Immunofluorescence micrographs show HeLa cells co-transfected with RIPK4-GFP and DVL2-FLAG for 36 h. Scale bars: 10 μm .

Supplementary Figure 11. RIPK4 overexpression in tumor cells can promote tumor growth.

A. Box and whisker plots indicate RIPK4 and cytoplasmic β -catenin levels after quantitation by densitometry of blots in Fig. 4B. Error bars represent the s.e.m (n=6 for non-cancerous, and n=9 for tumors). P-values calculated by student t-test.

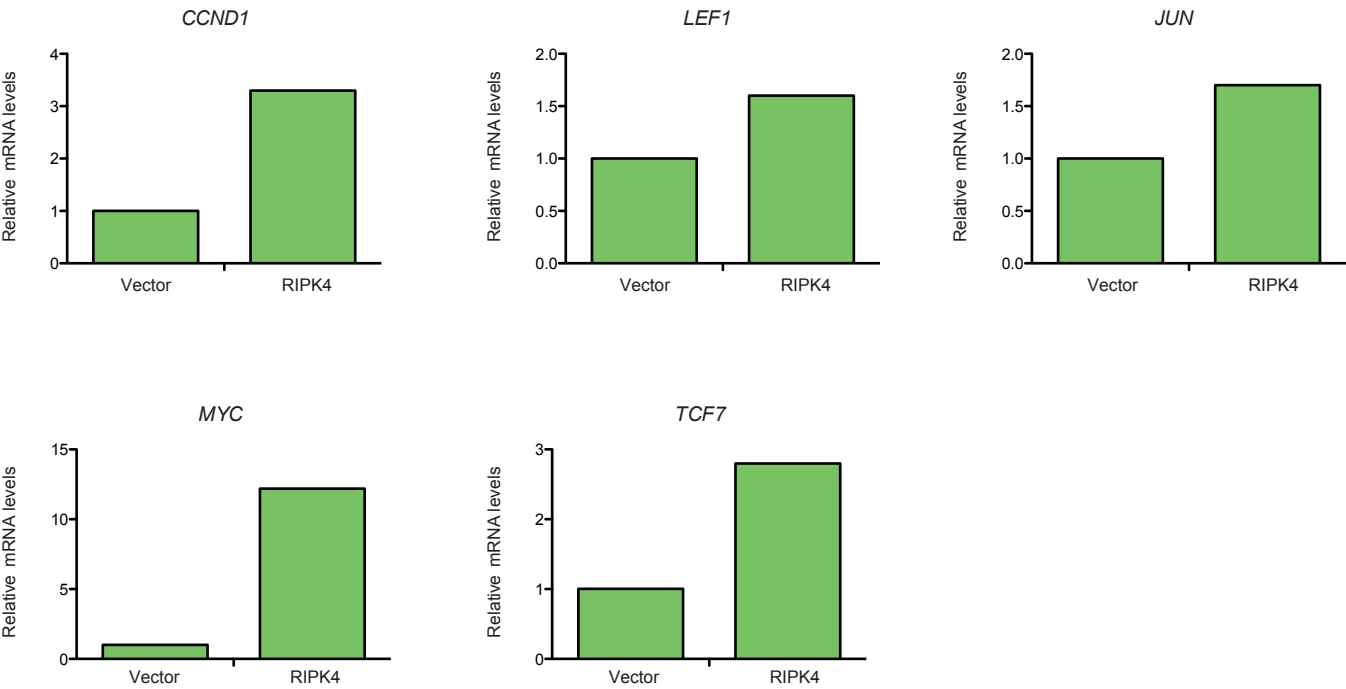
B. Western blots for RIPK4 indicate the degree of RIPK4 depletion from the N-TERA2 and HCT116 cells.

C. Expression of *GAD1* and *AXIN2* mRNAs in tumors from Fig. 4D (Error bars represent s.e.m. n=8).

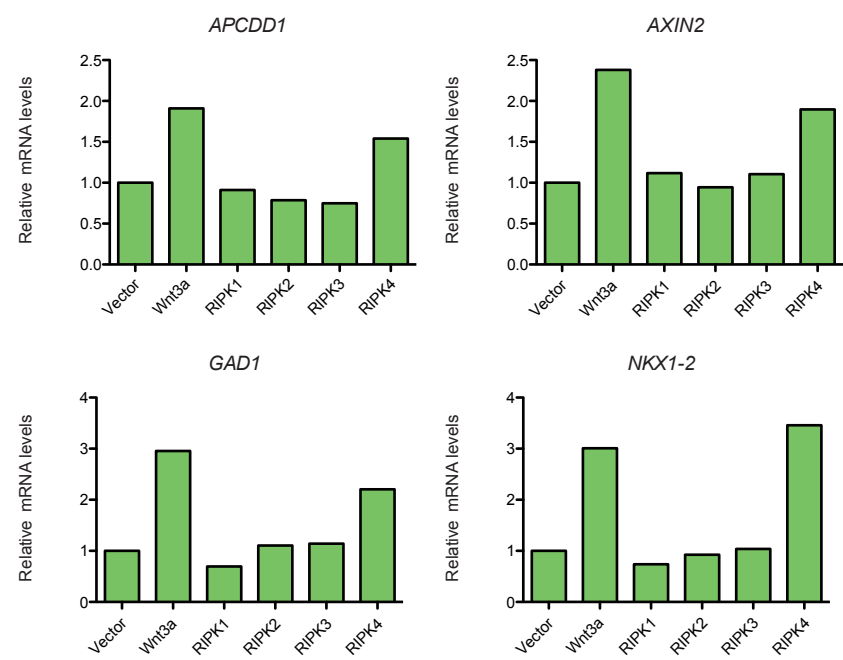
Supplementary Figure 12. A model for RIPK4 function.

Upon Wnt stimulation, RIPK4 phosphorylates DVL2 at Ser298 and Ser480, promoting the accumulation of cytosolic β -catenin and transcription of target genes.

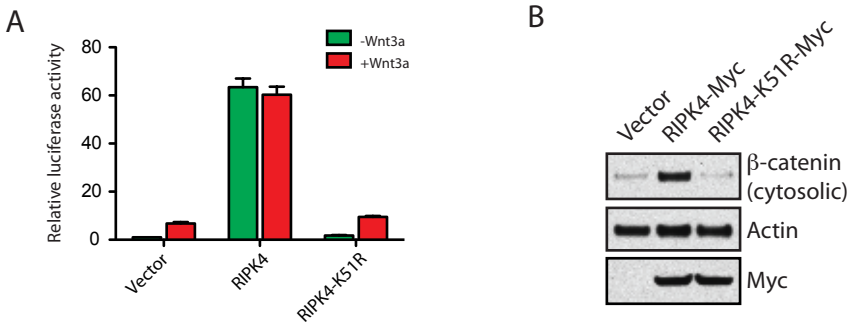
Supplementary Figure 1. Expression of RIPK4 in 293T cells upregulates Wnt target genes.



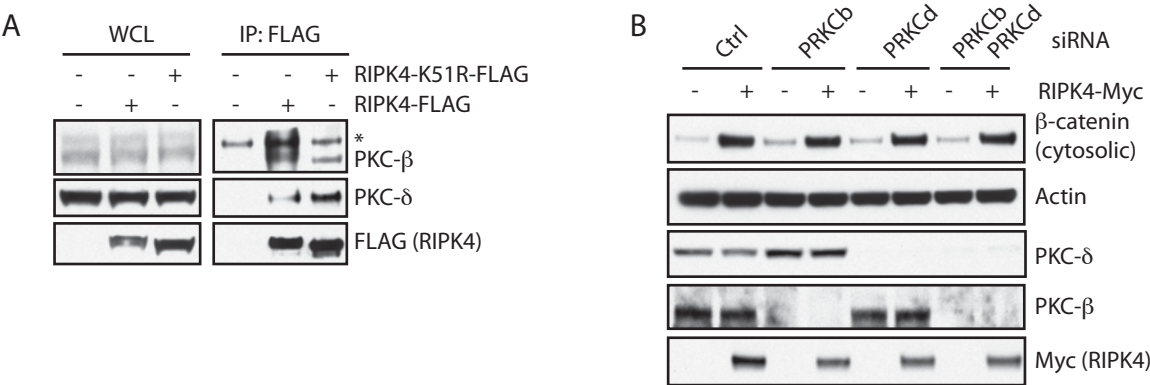
Supplementary Figure 2. Expression of RIPK4 in PA-1 cells upregulates Wnt target genes.



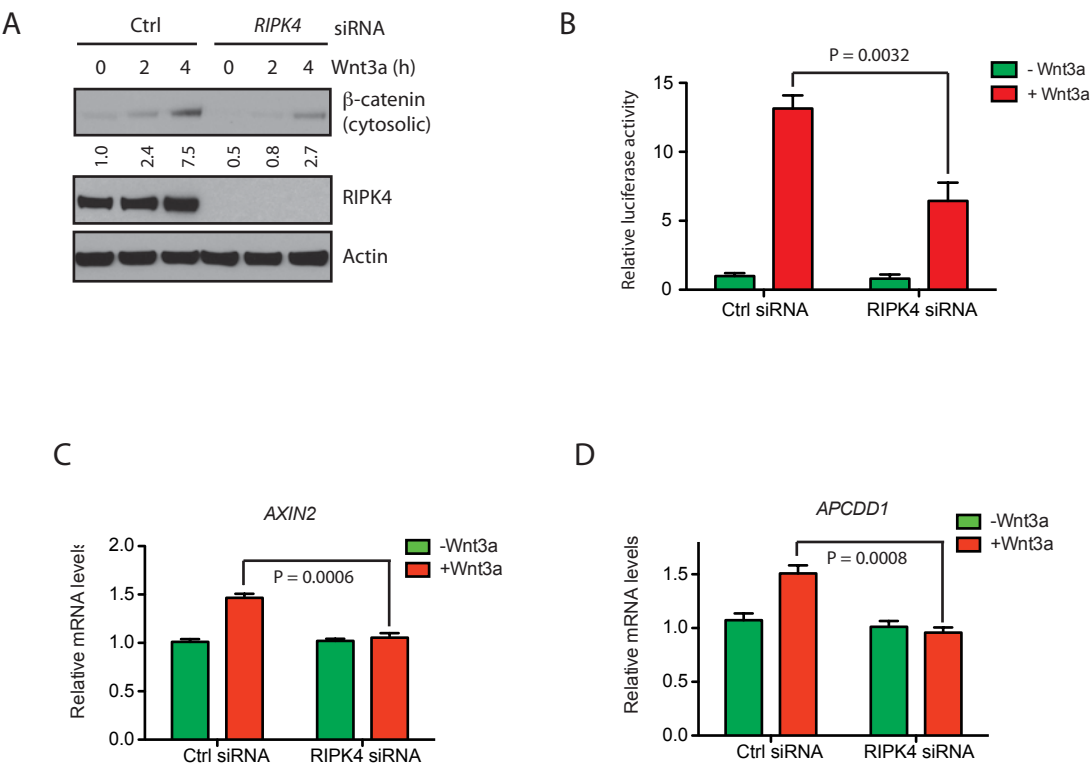
Supplementary Figure 3. RIPK4 requires a functional kinase domain to activate the Wnt pathway.



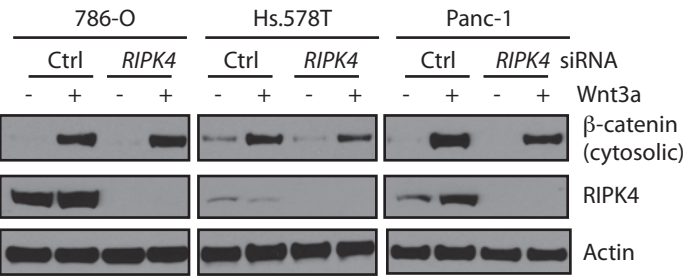
Supplementary Figure 4. Wnt pathway activation by RIPK4 occurs independently of PKC.



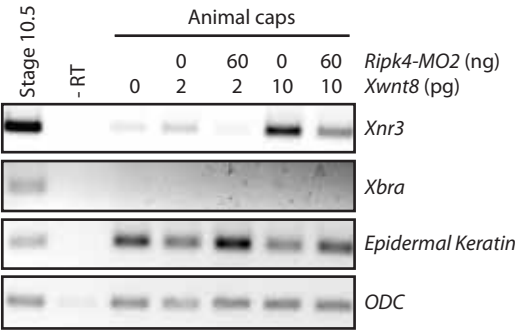
Supplementary Figure 5. Depletion of RIPK4 compromises Wnt signaling in 293T cells.



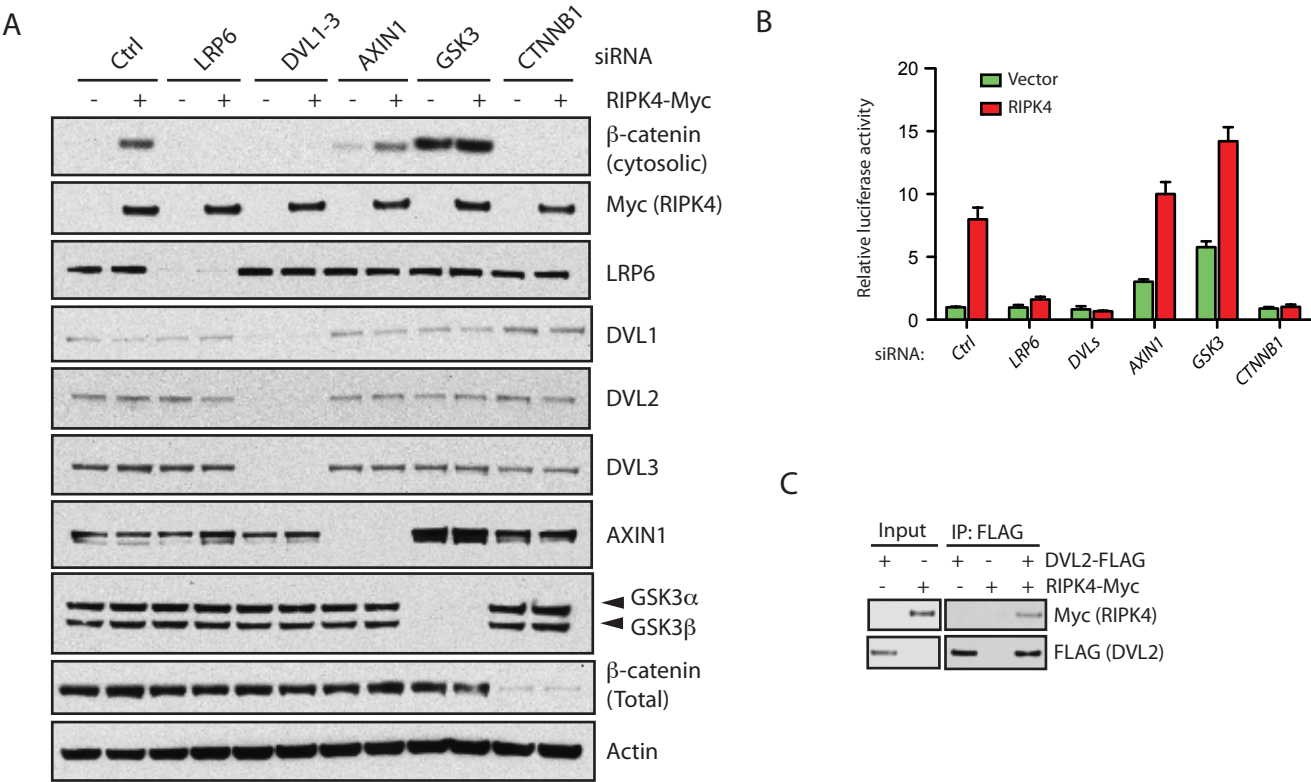
Supplementary Figure 6. Depletion of RIPK4 from 786-O, Hs.578T, and Panc-1 cells has no effect on Wnt3a-induced accumulation of cytosolic β -catenin.



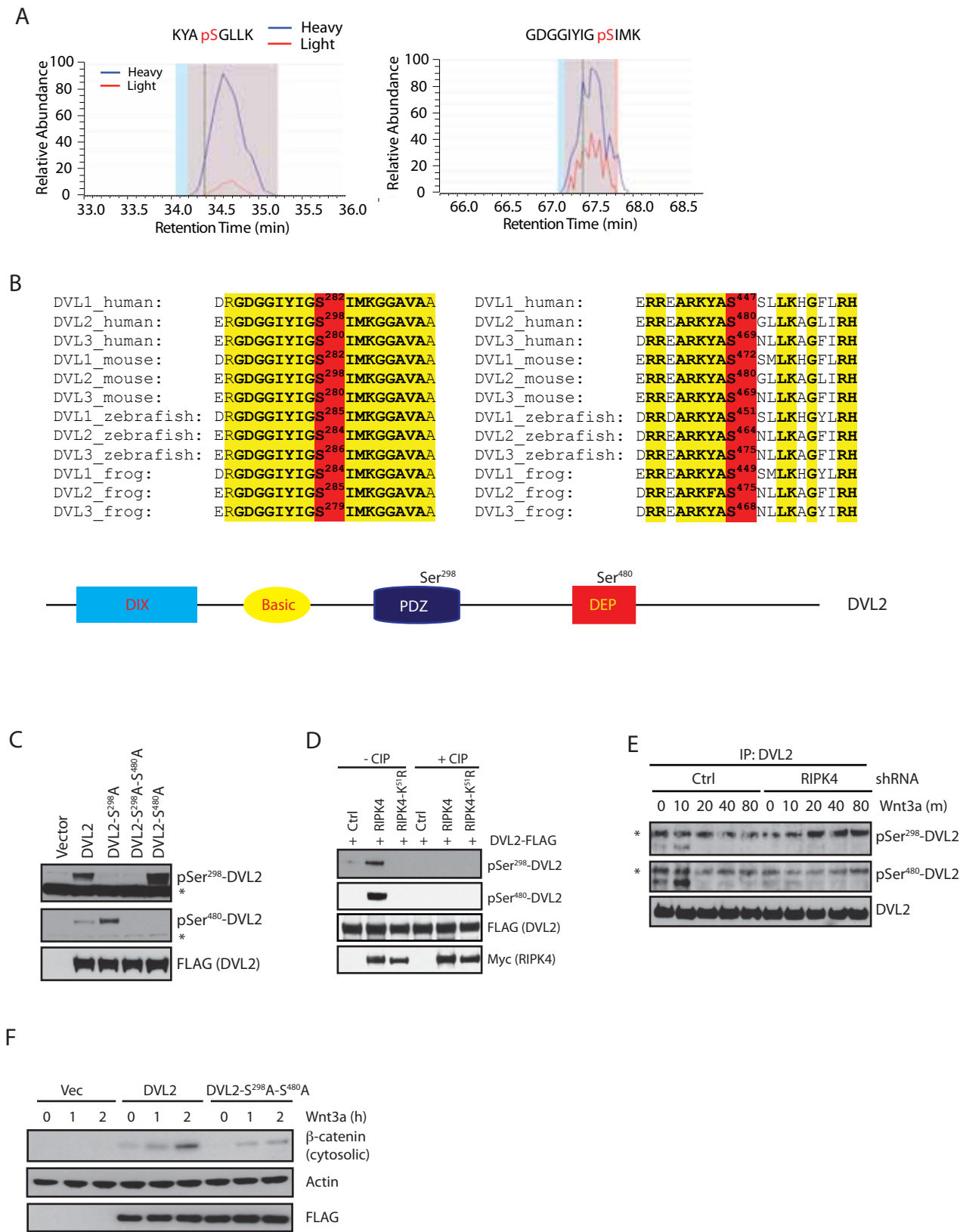
Supplementary Figure 7. Modulation of Wnt signaling in *Xenopus* embryos by Ripk4.



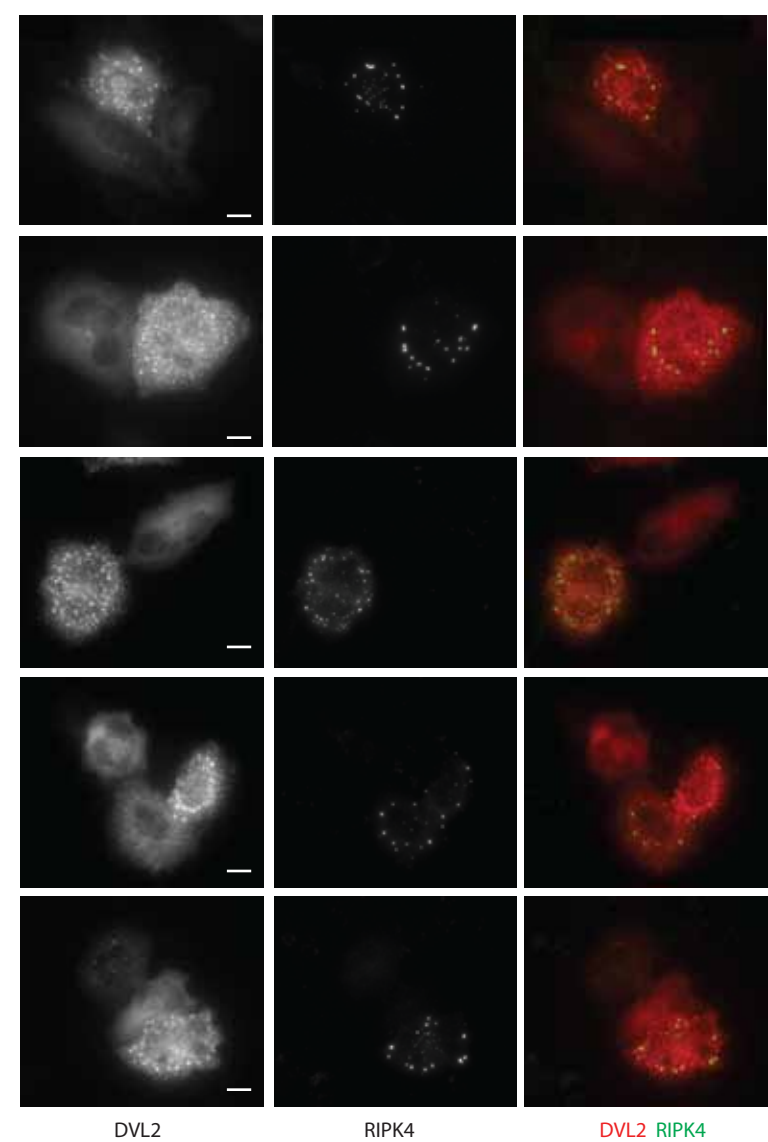
Supplementary Figure 8. DVLs and LRP6 are required for RIPK4 overexpression to cause the accumulation of cytosolic β -catenin.



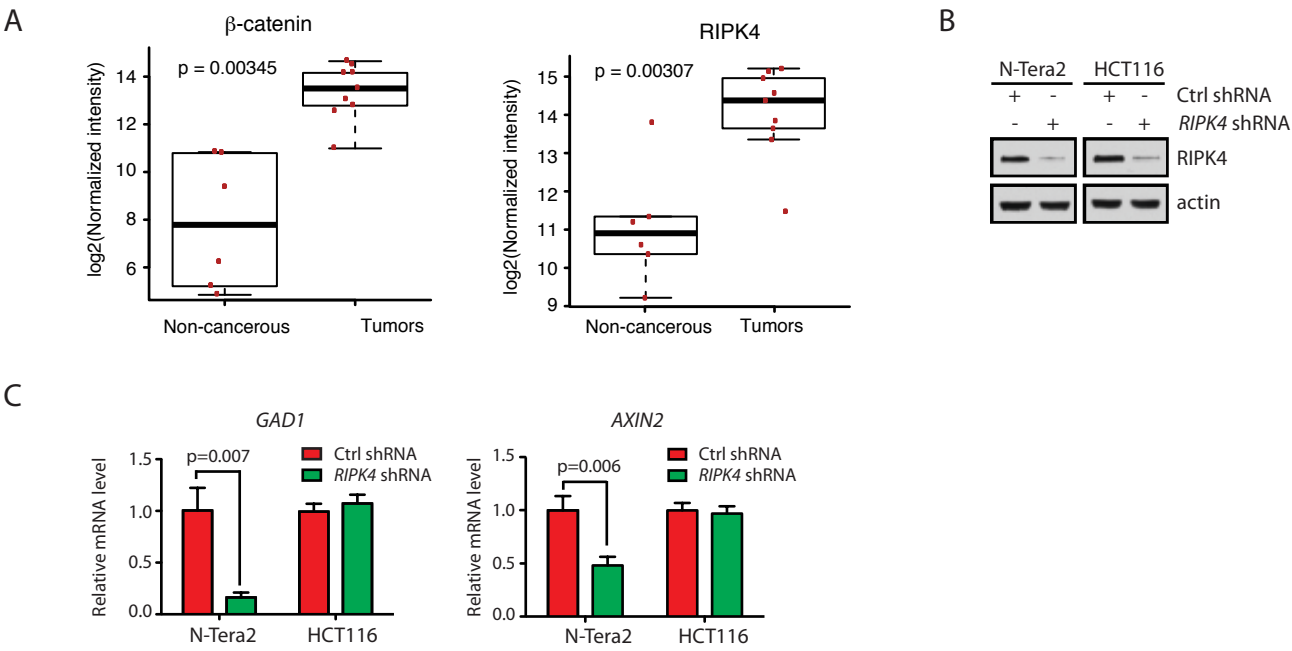
Supplementary Figure 9. Phosphorylation of DVL2 Ser298 and Ser480 by RIPK4.



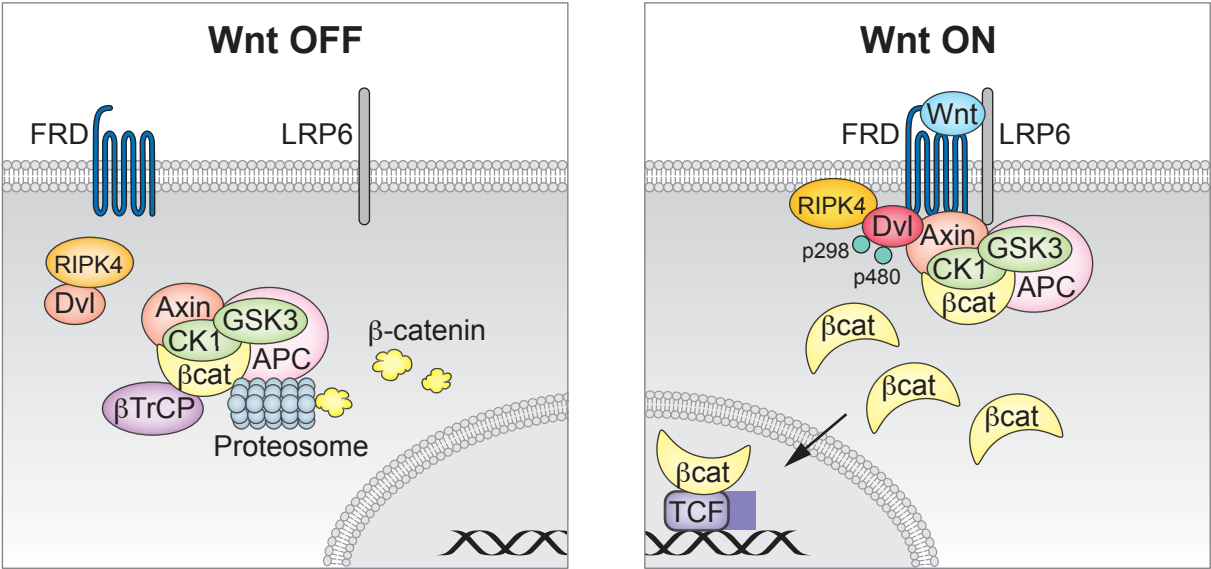
Supplementary Figure 10. RIPK4 expression redistributes DVL2 into puncta in HeLa cells.



Supplementary Figure 11. RIPK4 overexpression in tumor cells can promote tumor growth.



Supplementary Figure 12. A model for the RIPK4 function.



Supplementary Table 1. List of siRNA and shRNA sequences and sources used in this study

Genes	Gene ID	siRNA name	Source	Catalog No.	Sense sequence
<i>hRIPK4</i>	54101	RIPK4-1	Ambion	s28865	GCACGAUGUAUACAGCUUUtt
		Lentiviral shRIPK4	Sigma	TRCN0000007134	CCACGTCAAGATTTCTGATTT
		GIPZ lentiviral RIPK4	Open Biosystems	V3LHS_403697	GGACGCGCCCTCCTTATCCACCATA
<i>LRP6</i>	4040	<i>LRP6</i>	Ambion	s8291	GGCUACAAAUGUUCaucGAtt
<i>DVL1</i>	1855	<i>DVL1</i>	Dharmacon	J-004068-10	GCGAGUUCUUCGUGGACAU
<i>DVL2</i>	1856	<i>DVL2</i>	Dharmacon	J-004069-09	CCACAAUGUCUCUCAUAU
<i>DVL3</i>	1857	<i>DVL3</i>	Ambion	s675	GAUAUGUUGUACAGGUAAtt
<i>DVL3</i>	1857	<i>shDVL3</i>	Open Biosystems	TRCN0000097294	AAACCCAGGGCTGCCTTGAAAAAG
<i>AXIN1</i>	8312	<i>AXIN1-1</i>	Ambion	s15814	GAAAGUACAUUCUUGAUAAtt
		<i>AXIN1-2</i>	Ambion	s15815	GGGAUAAGCCUGUUCAGGAtt
		<i>AXIN1-3</i>	Ambion	s15816	GGAUACCUGCCGACCUUAAtt
<i>GSK3a</i>	2931	<i>GSK3a</i>	Ambion	s6236	GAAAGACGAGCUUUACCUAtt
<i>GSK3b</i>	2932	<i>GSK3b</i>	Ambion	s6241	GCUAGAUCACUGUAACAUAtt
<i>CTNNB1</i>	1499	<i>CTNNB1</i>	Ambion	s436	GGACCUAUACUACGAAAAtt
<i>PRKCB1</i>	5579	<i>PRKCB1</i>	Dharmacon	LQ-00375814	CCUGUCAGAUCCCUACGUA
<i>PRKCD</i>	5580	<i>PRKCD</i>	Ambion	s11099	GGGACACUAUAUCCAGAAtt
<i>GFP</i>	7011691	shGFP	Sigma	SHC004	CGTGATCTTCACCGACAAGAT
Control siRNA			Dharmacon	S-005000-01	TGGTTTACATGTTGTGTGA

References and Notes

1. P. Holland *et al.*, RIP4 is an ankyrin repeat-containing kinase essential for keratinocyte differentiation. *Curr. Biol.* **12**, 1424 (2002). [doi:10.1016/S0960-9822\(02\)01075-8](https://doi.org/10.1016/S0960-9822(02)01075-8) [Medline](#)
2. E. Kalay *et al.*, Mutations in RIPK4 cause the autosomal-recessive form of popliteal pterygium syndrome. *Am. J. Hum. Genet.* **90**, 76 (2012). [doi:10.1016/j.ajhg.2011.11.014](https://doi.org/10.1016/j.ajhg.2011.11.014) [Medline](#)
3. K. Mitchell *et al.*, Exome sequence identifies RIPK4 as the Bartsocas-Papas syndrome locus. *Am. J. Hum. Genet.* **90**, 69 (2012). [doi:10.1016/j.ajhg.2011.11.013](https://doi.org/10.1016/j.ajhg.2011.11.013) [Medline](#)
4. Y. Zhang *et al.*, Inhibition of Wnt signaling by Dishevelled PDZ peptides. *Nat. Chem. Biol.* **5**, 217 (2009). [doi:10.1038/nchembio.152](https://doi.org/10.1038/nchembio.152)
5. H. Clevers, R. Nusse, Wnt/ β -catenin signaling and disease. *Cell* **149**, 1192 (2012). [doi:10.1016/j.cell.2012.05.012](https://doi.org/10.1016/j.cell.2012.05.012) [Medline](#)
6. A. P. McMahon, R. T. Moon, Ectopic expression of the proto-oncogene int-1 in *Xenopus* embryos leads to duplication of the embryonic axis. *Cell* **58**, 1075 (1989). [doi:10.1016/0092-8674\(89\)90506-0](https://doi.org/10.1016/0092-8674(89)90506-0) [Medline](#)
7. W. T. Montross, H. Ji, P. D. McCrea, A beta-catenin/engrailed chimera selectively suppresses Wnt signaling. *J. Cell Sci.* **113**, 1759 (2000). [Medline](#)
8. R. McKendry, S. C. Hsu, R. M. Harland, R. Grosschedl, LEF-1/TCF proteins mediate wnt-inducible transcription from the *Xenopus* nodal-related 3 promoter. *Dev. Biol.* **192**, 420 (1997). [doi:10.1006/dbio.1997.8797](https://doi.org/10.1006/dbio.1997.8797) [Medline](#)
9. K. Satoh *et al.*, Anteriorization of neural fate by inhibitor of beta-catenin and T cell factor (ICAT), a negative regulator of Wnt signaling. *Proc. Natl. Acad. Sci. U.S.A.* **101**, 8017 (2004). [doi:10.1073/pnas.0401733101](https://doi.org/10.1073/pnas.0401733101) [Medline](#)
10. T. Schwarz-Romond, C. Merrifield, B. J. Nichols, M. Bienz, The Wnt signalling effector Dishevelled forms dynamic protein assemblies rather than stable associations with cytoplasmic vesicles. *J. Cell Sci.* **118**, 5269 (2005). [doi:10.1242/jcs.02646](https://doi.org/10.1242/jcs.02646) [Medline](#)
11. P. Polakis, Wnt signaling and cancer. *Genes Dev.* **14**, 1837 (2000). [Medline](#)
12. V. I. DeAlmeida *et al.*, The soluble wnt receptor Frizzled8CRD-hFc inhibits the growth of teratocarcinomas in vivo. *Cancer Res.* **67**, 5371 (2007). [doi:10.1158/0008-5472.CAN-07-0266](https://doi.org/10.1158/0008-5472.CAN-07-0266) [Medline](#)
13. M. N. Kitaeva *et al.*, Mutations in beta-catenin are uncommon in colorectal cancer occurring in occasional replication error-positive tumors. *Cancer Res.* **57**, 4478 (1997). [Medline](#)
14. R. M. Harland, In situ hybridization: an improved whole-mount method for *Xenopus* embryos. *Methods Cell Biol.* **36**, 685 (1991). [doi:10.1016/S0091-679X\(08\)60307-6](https://doi.org/10.1016/S0091-679X(08)60307-6) [Medline](#)
15. T. D. Wu, S. Nacu, Fast and SNP-tolerant detection of complex variants and splicing in short reads. *Bioinformatics* **26**, 873 (2010). [doi:10.1093/bioinformatics/btq057](https://doi.org/10.1093/bioinformatics/btq057) [Medline](#)
16. S. Anders, W. Huber, Differential expression analysis for sequence count data. *Genome Biol.* **11**, R106 (2010). [doi:10.1186/gb-2010-11-10-r106](https://doi.org/10.1186/gb-2010-11-10-r106) [Medline](#)
17. M. Mann, Functional and quantitative proteomics using SILAC. *Nat. Rev. Mol. Cell Biol.* **7**, 952 (2006). [doi:10.1038/nrm2067](https://doi.org/10.1038/nrm2067) [Medline](#)